Journal of Food Biochemistry

SPECIAL ISSUE Biochemical innovations in food waste valorization

WILEY

RESEARCH ARTICLE OPEN ACCESS

Valorization of Purple Prickly Pear Peel By-Products: Antiproliferative and Pro-Apoptotic Effects on Human Colorectal Cancer Cells HCT116

Yasmany Armas Diaz[1,2,3,4] | Zexiu Qi[1,2,3,4] | Bei Yang[1,2,3,4] | Danila Cianciosi[1,2,3,4] | Luca Mazzoni[5] | Massimiliano Gasparrini[5] | Tamara Y. Forbes Hernandez[6] | José L. Quiles[7] | Rubén Calderón Iglesias[8,9,10] | Maurizio Battino[1,2,3,4,8,11] | Francesca Giampieri[1,2,3,4,8]

[1]Department of Clinical Sciences, Polytechnic University of Marche, Ancona, Marche, Italy | [2]Joint Laboratory on Food Science, Nutrition, and Intelligent Processing of Foods, Polytechnic University of Marche, Ancona, Marche, Italy | [3]Universidad Europea del Atlántico, Santander, Cantabria, Spain | [4]Jiangsu University, Zhenjiang, Jiangsu, China | [5]Department of Agricultural, Food and Environmental Sciences, Università Politecnica delle Marche, Ancona, Marche, Italy | [6]Dipartimento di Scienze Biomediche, Università degli Studi di Cagliari, Cagliari, Sardegna, Italy | [7]Department of Physiology, Institute of Nutrition and Food Technology "José Mataix Verdú", Biomedical Research Centre, University of Granada, Armilla, Andalusia, Spain | [8]Research Group on Food, Nutritional Biochemistry and Health, Universidad Europea del Atlántico, Santander, Cantabria, Spain | [9]Universidade Internacional do Cuanza, Cuito, Bié, Angola | [10]Universidad de La Romana, La Romana, La Romana, Dominican Republic | [11]International Joint Research Laboratory of Intelligent Agriculture and Agri-Products Processing, Jiangsu University, Zhenjiang, Jiangsu, China

Correspondence: Maurizio Battino (m.a.battino@staff.univpm.it)

Received: 14 November 2025 | **Revised:** 3 April 2026 | **Accepted:** 9 May 2026

Guest Editor: Prisca-Maryla Henheik

Keywords: antiproliferative | cell cycle arrest | colorectal cancer | *Opuntia ficus-indica* peel | proapoptotic

ABSTRACT

Opuntia ficus-indica peel is known to possess antioxidant, anti-inflammatory, and anticancer activities and currently is discarded or used for animal feeding. Within this context, the aim of this work was to evaluate the antiproliferative and pro-apoptotic effect of purple prickly pear peel extract (PPE) on the human colon adenocarcinoma cancer cell line (HTC116). The methanolic extract of PPE was characterized in terms of betalain and polyphenols as well as total antioxidant capacity. Cell viability, apoptosis induction, cell cycle arrest, and reactive oxygen species (ROS) production assays were performed. Important proteins and genes related to proliferation and apoptosis were determined. PPE represents a good source of bioactive compounds with a high antioxidant capacity. Cell viability was reduced gradually by PPE treatments, with lower effects in nontumorigenic cells. Compared to the control group, a significant induction of apoptosis as well as cell cycle arrest in the sub-G1 phase and ROS production was observed in PPE-treated cells. Furthermore, the treatment induced the overexpression of p53 at protein levels and upregulated the mRNA expression of pro-apoptotic BAX, CASP9, BID, and CYCS, along with the significant decrease of anti-apoptotic BCL2 gene expression. Simultaneously, cyclin D1 and CDK4 gene expression were significantly decreased, while p21 increased considerably. The treatment also induced the downregulation of Her2 and PI3K at protein levels and caused the suppression of PI3KCA and mTOR expression at gene levels. Overall, these findings suggested that PPE has potential anticancer effects against human colon adenocarcinoma progression.

Yasmany Armas Diaz and Zexiu Qi equally contributed.

1 | Introduction

Cancer is considered a predominant cause of death and unfortunately represents an important barrier to increased life expectancy around the world. Specifically, colorectal cancer (CRC) is the third most common and the second cause of cancer mortality worldwide [1]. Even though great efforts have been made in treatment methods, there is still a high rate of mortality among CRC patients that is associated with poor prognosis and metastasis [2]. The most widely used treatments for CRC include surgery combined with radiotherapy and/or chemotherapy [3]. However, in the last decade, many scientific studies have demonstrated the positive effect of combining the most common cancer treatments with natural compounds due to the enhancing of apoptosis induction, reduction of cell proliferation, and, in several cases, overcoming drug resistance [4, 5].

The consumption of natural products has gained increasing attention due to their richness in bioactive components, including phenolic acids (e.g., piscidic and eucomic acids), flavonoids (e.g., isorhamnetin and kaempferol), betalains (betanin and indicaxanthin), and vitamins, which are associated with multiple pharmacological actions such as antioxidant, anti-inflammatory, cardioprotective, and antitumor [6–8]. In vitro, in vivo, and clinical studies have shown that natural compounds possess excellent anticancer effects, and at the same time, they present advantages with respect to drugs, including low toxicity, few side effects, and lower cost of production [9–11].

Opuntia is a genus of the cactus family, Cactaceae, and several species have been reported, but the most highly cultivated and domesticated is *Opuntia ficus-indica* (OFI) [12]. *Opuntia* species are distributed mainly in Mexico and Latin America, as well as South Africa and central Mediterranean countries, such as Italy and Spain [13]. The second largest producer around the world is Italy, after Mexico, and the cultivation is mainly located in Sicily [14]. *O. ficus-indica*, commonly called prickly pear, possesses several health benefits, including antimicrobial, anticancer, and anti-inflammatory properties [15, 16]. The most significant bioactive components found in OFI are betaxanthin, betacyanin, and phenolic compounds, such as phenolic acids and flavonoids, namely kaempferol, isorhamnetin, and quercetin derivatives [17]. Previous studies have demonstrated the antiproliferative effect of OFI extracts in breast, liver, and CRC cell lines [15].

The researchers have been focused mainly on the prickly pear pulp as a source of bioactive compounds; however, it is important to highlight that several studies have shown that peels contain significant amounts of bioactive compounds and sometimes even more than pulp [18–20]. The prickly pear peel is commonly discarded or used as fodder [21]. It is well-known that the valorization of agricultural by-products has prominent effects on minimizing the negative environmental impact, lowering the costs of managing waste and improving social sustainability. In general, there is little scientific information about the incidence of prickly pear intake in the human body, despite there being a lot of information about its chemical composition [17].

This study aimed to investigate the antiproliferative and pro-apoptotic effects of bioactive compounds from purple prickly pear peel on the human colon adenocarcinoma cell line (HCT116) in order to explore its potential for valorization.

2 | Materials and Methods

2.1 | Chemicals and Reagents

Unless different information is explicitly given in writing, chemicals and reagents were acquired from Merck (Milan, Italy), and the purity grade was the highest available at the time. Media (McCoys's 5A and Eagle's Minimum Essential Medium [EMEM]), fetal bovine serum (FBS), and antibiotic–antimycotic (100x) were obtained from Thermo Fisher Scientific (Milan, Italy). Primary and secondary antibodies were purchased from Santa Cruz Biotechnology and Antibodies.com, and primers were from SIAL (Rome, Italy).

2.2 | Plant Material and Sample Preparation

Prickly pear (*O. ficus-indica*) fruit has been kindly supported by Euroagrumi-Catania (Sicily, Italy). The local genotype selected for this study was the red-skinned one. The samples were collected in August 2022, approximately at 50% "color break" because this is where Brix (11.2–16.4) [22] and firmness are optimum in this nonclimacteric fruit. After picking, the fruits were immediately transported to the laboratory, put at 4°C, and processed within 3 days after harvesting. Twenty ripe fruits were selected for further analysis. Fresh fruits were cleaned thoroughly, paying special attention to the hair-like thorns (glochids) that cover them. The glochids were removed by brushing under cold running water while holding with tongs. Next, the pulp and peel were removed from each other; the peels were chopped into small pieces and freeze-dried for 5 days at −45°C and 3.7×10^{-6} MPa. Finally, samples were pulverized using an IKA A11 basic analytical mill to obtain a fine and homogeneous powder, and the powder was stored at −80°C until further analysis.

2.3 | Methanolic Extract Preparation

The freeze-dried purple prickly pear peel powders were mixed with 80% aqueous methanol (1:50 w/v), then immersed in a water ultrasonic bath (SONICA, 40 kHz/180 W) with cold water for 15 min and afterward 45 min of stirring at room temperature (RT) in the dark [23]. The liquid was recovered, and the extraction was repeated twice with 30% of the solvent and 15 min of stirring. After extractions, the mixtures were centrifuged (3500 rpm, 10 min, 4°C) and filtered using 0.45 μm mixed cellulose ester filters and collected in an amber vial. For further experiments, the extracts were obtained in triplicate, and for the analysis with cells, the filtrate was concentrated under reduced pressure at 35°C.

2.4 | Phytochemical Characterization

2.4.1 | Betalains

The methodology to extract the betalains is similar to the one described previously in Section 2.3, but instead of 80% methanol, Milli-Q water was used [24]. Betalains' absorbance was analyzed directly from the aqueous extract. The samples were analyzed at 538 nm for betacyanin (betanin) detection using a microplate reader (Infinite® 200 PRO, Tecan, Austria). Betalain content was calculated from the interpolation on a calibration curve [25]. The final results were expressed in milligrams of betanin equivalents per gram of dry weight (DW) (mg BetEq/g DW).

2.4.2 | Total Phenolic Content (TPC) Assay

Total polyphenols were assessed using the Folin–Ciocalteu colorimetric method, in accordance with the work of Slinkard and Singleton [26] with slight modifications. Briefly, diluted samples or standards (100 μL) were mixed with 500 μL of Folin reagent, followed by 5 min incubation at RT. After 400 μL of sodium carbonate (0.7 M) was added, the solution was vortexed thoroughly and incubated in the dark at RT for 2 h. Finally, the specific absorbance was recorded at 760 nm using a microplate reader (Infinite® 200 PRO, Tecan, Austria). The results were expressed as milligrams of gallic acid equivalents per gram of DW (mg GAEq/g DW).

2.4.3 | Total Flavonoids Assay

The flavonoid content was measured using the aluminum trichloride method, with slight adaptations from the protocol described by Zhishen et al. [27]. Shortly, 200 μL of the extracts or standards (catechin) were added to Milli-Q water (220 μL) and 60 μL of sodium nitrite (5%) and incubated for 6 min. Then, 120 μL of aluminum chloride hexahydrate (10%) was added, and 5 min later, 400 μL of sodium hydroxide (1 M) was mixed vigorously. The absorbance of this final solution was recorded at 700 nm using a microplate reader (Infinite® 200 PRO, Tecan, Austria). Flavonoid content was expressed as milligrams of catechin equivalents per gram of DW (mg CatEq/g).

2.4.4 | Ascorbic Acid (AsA) Quantification

AsA content was assessed by high-performance liquid chromatography (HPLC) following slight modifications to the method described previously by Davey et al. [28]. The HPLC system was equipped with a C18 column (Rx-C18, 4.6 × 100 mm, 3.5 μM, Agilent 861 967–902). The mobile phase consisted of sodium dihydrogen phosphate (0.1 M) and ethylenediaminetetraacetic acid (0.2 mM, pH = 3.1) with a flow rate of 0.7 mL/min, and the detection was with a UV detector at 254 nm. AsA content was calculated by finding its response on the curve and interpolating the corresponding concentration of AsA and the final results were expressed as mg of AsA/g DW.

2.4.5 | Identification and Quantification of Polyphenols

The purple prickly pear peel methanolic extract was analyzed following the protocol previously described by Mata et al. [17], slightly modified. The HPLC–ESI–QTOF–MS/MS system consisted of an Agilent 6540 Ultra High Definition (UHD) Accurate Mass Q-TOF detector equipped with a dual ESI Jet Stream interface coupled with an Agilent 1260 series liquid chromatograph equipped with a microvacuum degasser, binary pump, thermostatted autosampler and column compartment, and diode array detector. The method was performed on an Agilent Zorbax Eclipse Plus C18 column with dimensions of 4.6 × 150 mm and a particle size of 1.8 μm maintained at 25°C. The mobile phases consisted of 0.1% formic acid (FA) as phase A and acetonitrile with 0.1% FA as phase B, with the following gradient: 0 min, 5% phase B; 5 min, 70% phase B; 45 min, 95% phase B; 50 min, 5% phase B; and finally, a 5 min conditioning cycle with the initial analysis conditions. The flow rate was set at 0.5 mL/min and 5 μL as the injection volume.

Q-TOF used for detection was performed in negative ionization mode in a mass range of 50–1700 m/z. The gas used for ionization and drying was ultrapure N_2, and the temperature was set at 325°C and 400°C, with flows of 10 and 12 L/min, respectively. Additionally, MS/MS analyzes were performed in automatic fragmentation mode. All data acquisition operations were managed by Masshunter workstation software version B.06.00 (Agilent Technologies).

The tentative identification of the detected compounds was based on the molecular formula obtained from the exact mass and isotopic distribution data and the retention times and fragmentation patterns recorded, and data were compared, whenever possible, with scientific literature regarding *Opuntia* spp. The identified elements were quantified using surrogate standards; the surrogate analytical standards and main analytical parameters for quantification of samples are summarized in Table S1.

The main polyphenol compounds identified and quantified included phenolic acids (e.g., eucomic and piscidic acids) and flavonoids (e.g., isorhamnetin); detailed results are reported in Section 3.1.1.

2.5 | Reducing Capacity and Radical Scavenging Assays

The antioxidant activity was measured considering the most common mechanism, hydrogen-donating or radical-scavenging ability. To achieve this, four assays were performed: ferric reducing antioxidant power (FRAP), 1,1-diphenyl-2-picrylhydrazyl (DPPH), Trolox equivalent antioxidant capacity (TEAC), and oxygen radical absorbance capacity (ORAC).

2.5.1 | FRAP Assay

The FRAP assay was carried out based on the protocol proposed by Deighton [29]. Briefly, the FRAP solution was prepared by putting together 10 volumes of sodium acetate (25 mM, pH 3.6), 1 volume of 2,4,6-tripyridyl-s-triazine (TPTZ) (10 mM in HCl [40 mM]), and 1 volume of ferric chloride hexahydrate (20 mM) aqueous solution; this solution was prepared just before starting the assay. Then, 900 μL of FRAP reagent was mixed with 100 μL of standards or samples; the mix was vortexed and incubated for 4 min, following reading the absorbance at 593 nm using a microplate reader (Infinite® 200 PRO, Tecan, Austria). Antioxidant capacity was determined using a calibration curve generated with a Trolox standard, and final results were expressed as micromoles of Trolox equivalents per gram of DW (μmol TxEq/g DW).

2.5.2 | DPPH Radical-Scavenging Activity

This analysis was conducted following the method described by Kitts, Wijewickreme, and Hu [30] with slight modifications. First, 400 μL of DPPH solution prepared at 0.2 mM in methanol was mixed with 550 μL of ethanol (70%) and 80 μL of sample or standards, and the mix was strongly vortexed. Then they were incubated in the dark for 1 h, and finally, the absorbance was measured at 517 nm using a microplate reader (Infinite® 200 PRO, Tecan, Austria). The antioxidant activity was obtained after making a calibration curve plotting Trolox standard concentrations against inhibition of absorbance (%), and the final results

were expressed as micromoles of Trolox equivalents per gram of DW (μmol TxEq/g DW).

2.5.3 | TEAC Assay

The methodology followed to perform this assay was reported by Re et al. [31] with minor modifications. The ABTS radical cation ($ABTS^{\bullet+}$) was produced by direct reduction of ABTS (7 mM) and potassium persulfate (140 mM) in the dark for around 12 h at RT. Just before the analysis, the $ABTS^{\bullet+}$ solution was diluted with ethanol with the purpose of ensuring the absorbance values were within 0.6 and 0.9. Then, 1 mL of $ABTS^{\bullet+}$ solution diluted was mixed with 10 μL of samples or Trolox standards, vortexed vigorously, and kept in the dark for 3–5 min. The absorbance was measured at 734 nm using a microplate reader (Infinite® 200 PRO, Tecan, Austria). The absorbance values were converted to inhibition of absorbance (%), and a standard curve was obtained using Trolox. The scavenging capacity was finally expressed as micromoles of Trolox equivalents per gram of DW (μmol TxEq/g DW).

2.5.4 | ORAC Assay

The methodology for ORAC was carried on with some modifications proposed by Smeriglio et al. [32]. The analysis was performed in a 96-well microplate. In each well were added 150 μL of fluorescein (0.08 μM) and 25 μL of samples or standards diluted previously in phosphate buffer (pH = 7.4) and incubated for 10 min at 37°C. Then, 25 μL of 2,2′-azobis(2-amidinopropane) dihydrochloride (AAPH) (180 mM) was added to produce the radicals. Then, the plate was shaken for 5 s, and the fluorescence was recorded every 2 min for a total of 80 min with emission and excitation wavelengths of 530 and 485 nm, respectively. The microplate reader (Infinite® 200 PRO, Tecan, Austria) was maintained at 37°C. The ORAC values were calculated as the area under the curve, and the final scavenging capacity was expressed as micromoles of Trolox equivalent per gram of DW (μmol TxEq/g of DW).

2.6 | Cell Culture

Human colon adenocarcinoma (HCT116) and human normal colon fibroblast (CCD-18Co) cell lines were obtained from the American Type Culture Collection (ATCC, Manassas, VA, USA). HCT 116 cells were cultured in McCoy's 5A and CCD-18Co in EMEM. All media were prepared with heat-inactivated FBS at 10% and 1% antibiotic–antimycotic (10,000 units/mL of penicillin, 10,000 μg/mL of streptomycin, and 25 μg/mL of amphotericin B). All cell lines were cultured at 37°C in a humidified atmosphere (95% air, 5% CO_2), and all the experiments were conducted with cells between passages 4 and 12. The culture medium was replaced three times a week.

2.7 | Cell Viability Assay

Cell viability assessment was performed by using a standard colorimetric assay based on mitochondrial activity called MTT [33]. Cells were seeded into 96-well plates at a density of 5×10^3 cells/well using specific complete growth medium and allowing them to attach around 18–20 h. Then, the cells were treated with purple prickly pear peel extract (PPE) in a range of 0–15 mg/mL for 24, 48, and 72 h. The treatment was previously filtered with 0.2 μm Mixed Cellulose Esters microfilters. After the specific incubation times, 30 μL of RPMI medium containing 2 mg/mL of 3-(4,5-dimethylthiazol-2-yl)-2,5-diphenyltetrazolium bromide was added, and the cells were incubated for 2–3 h more. Next, the media were gently removed, and the produced formazan crystals were dissolved in 100 μL of dimethyl sulfoxide, and the absorbance was recorded at 590 nm in a microplate reader (INFINITI PRO 200, Austria). In all cases, the results were expressed in terms of % of cellular viability relative to control (cells treated with only media), and the concentrations of extract necessary to decrease 30%, 50%, and 70% of the cellular viability (IC_{30}, IC_{50}, and IC_{70}) were calculated. The selectivity index (SI) of PPE was estimated by dividing the IC_{50} values for the nontumorigenic cells by those obtained for the cancer cell line [34].

2.8 | Tali™ Image-Based Cytometer

All analyses using the Tali™ Image-Based Cytometer (Thermo Fisher Scientific, Milan, Italy) were evaluated considering PPE concentrations as the ones obtained after the MTT assay (4, 8, and 12 mg/mL), which are according to the IC_{30}, IC_{50}, and IC70, respectively. Negative control cells were grown only in media, and betanin (5 mM) was a positive control. Betalains, and specifically betanin, are usually found in high amounts in purple prickly pear extracts compared with other bioactive compounds. For that reason, betanin was used as a reference to elucidate whether the effect of peel extract is held mainly by its more abundant bioactive compound or it is a synergistic effect between all compounds present in the extract.

2.8.1 | Apoptosis Induction Assay

The apoptotic cells were detected by using the Tali™ Apoptosis Assay Kit–Annexin V Alexa Fluor® 488 (Thermo Fisher Scientific, Milan, Italy) following the manufacturer's instructions. HCT 116 cells were seeded at a density of 2.0×10^5 cells per well into 6-well plates and incubated overnight. The day after, the cells were exposed to increasing concentrations of PPE, media, or betanin (5 mM) and placed again in the incubator. Cells were harvested 48 h later by using trypsin, then collected, and the pellet was mixed back with 100 μL of Annexin V Binding Buffer (ABB). Immediately, 5 μL of Annexin V AlexaFluor®488 was added to this solution and kept in the dark for 20 min at RT. Next, pellets were harvested again by centrifugation, and 100 μL of ABB was added again, following 1 μL of propidium iodide (PI) to each sample. This solution was incubated from 2 to 5 min in the dark. Finally, cells were analyzed with the Tali™ Image-Based Cytometer that evaluated the percentage of live (Annexin V−/PI−), apoptotic (Annexin V+/PI), and dead (Annexin V+/PI+) cells. The results were expressed as fold change in treated cells in respect to the negative control.

2.8.2 | Cell Cycle Analysis

The Tali™ Cell Cycle Kit (Thermo Fisher Scientific, Milan, Italy) was used to calculate the percentage of cells in each phase of the cell cycle by combining PI, RNase A, and Triton X-100 using the Tali™ Image-Based Cytometer (Thermo Fisher Scientific, Milan, Italy) according to the manufacturer's instructions. Briefly, tumor cells were seeded overnight at a density of 3.0×10^5 cells per well into 6-well plates. The day after, cells were incubated with different concentrations of PPE, media, or betanin (5 mM). After

the treatment time (48 h), the cells were harvested by trypsinization, and the pellet was washed twice with cold phosphate-buffered saline (PBS). Then, cells were fixed with 70% cold ethanol at −20°C overnight. After the fixing time, pellets were washed twice with PBS and resuspended in 100 μL of PBS-based PI solution containing 0.2 mg/mL RNase A, 0.1% Triton® X-100, and 20 μg/mL PI. The mix was incubated for 30 min in the dark at RT. Finally, samples were analyzed in the Tali machine, and the percentage of cells in each phase was used as the final expression.

2.8.3 | Intracellular Reactive Oxygen Species (ROS) Production Assay

The CellROX® Oxidative Stress kit (ThermoFisher Scientific, Milan, Italy) was used to evaluate the intracellular ROS generation according to the manufacturer's instructions. Shortly, tumor cells were seeded at a density of 2.0×10^5 cells per well into 6-well plates and allowed to attach overnight. The next day, cells were exposed to increasing concentrations of PPE, media, or betanin (5 mM) and incubated for another 48 h. After the treatment time, the cells were detached by trypsinization, the pellet was washed with PBS and resuspended in 1 mL of complete media containing CellROX® Orange Reagent at a final concentration of 5 μM, and the tubes were incubated in the dark for 30 min at 37°C. Next, media were removed by centrifugation, and the pellets were resuspended in 100 μL of PBS. Then, cells were analyzed with the Tali™ Image-Based Cytometer. The machine displayed the results of the analysis as a percentage of red cells (intracellular ROS) after the automatic capture of images and analyzed them. The results were expressed as the intracellular ROS content fold increase in treated cells in respect to the control, and the percentage of cells in each phase was used as the final expression.

2.9 | RNA Isolation and Quantitative Real-Time-qPCR Analysis

Tumorigenic cells were seeded at a density of 3.0×10^6 in a T75 flask and allowed to attach overnight, then the cells were cultured with PPE (4, 8, and 12 mg/mL), only media, and betanin (5 mM), and the treatment lasted for 48 h. The isolation of RNA was done by using the PureLink RNA Mini Kit, following the protocol described by the manufacturer (Invitrogen, Milan, Italy). The purity and concentration of the RNA isolated were observed by employing the microplate spectrophotometer system. The obtained RNA was reverse-transcribed to complementary DNA (cDNA) applying the All-in-one 5X RT MasterMix with gDNA Removal kit (Applied Biological Materials Inc., Richmond, Canada), taking 100 μg of RNA for each sample. RT-qPCR was carried out by using the QuantStudio™ 1 Real-Time PCR System (ThermoFisher Scientific, Milan, Italy) according to the BlasTaq™ 2X qPCR MasterMix protocol (Applied Biological Materials Inc., Richmond, Canada). Primers used are shown in Table 1. Actin was utilized as a housekeeping gene, and relative quantification was calculated using the $2^{-\Delta\Delta ct}$ method as described elsewhere [35]. Final results are expressed as fold change relative to the control group.

2.10 | Western Blot Analysis

HCT116 cells were maintained in the incubator overnight after seeding, and then the different treatments were applied for 48 h. Increasing concentrations of PPE (4, 8, and 12 mg/mL), only media, and betanin (5 mM) were used. After treatment, cells were harvested, and the pellets lysed with RIPA buffer (50 mM Tris-HCl, pH 8.0, with 150 mM sodium chloride, 1.0% Igepal CA-630 [NP-40], 0.5% sodium deoxycholate, 0.1% sodium dodecyl sulfate, and 1x protease inhibitor cocktail [Roche]). The lysate was centrifuged for 30 min at 4°C; the supernatant was collected, and protein concentration was determined using the Bradford assay (Bio-Rad, Hercules, USA). Samples were diluted accordingly to load 30–50 μg of protein per lane on 7.5%–10% SDS–PAGE gels. Next, proteins were transferred onto a nitrocellulose membrane using the Trans-Blot Turbo transfer system (Bio-Rad, Milan, Italy). Membranes were blocked with 5% skim milk for 1 h at RT and incubated overnight at 4°C with primary antibodies against p53 (sc-6243) and HER2 (sc-134481) and PI3K (A94027) and actin (A309717). Following this, the membranes were incubated again for 1 h at RT with their specific conjugated secondary antibodies. At the end, chemiluminescent signals were captured with the C-DiGit Blot Scanner (LICOR, Bad Homburg, Germany), and band intensities were quantified using Image Studio Digits software 3.1 (C-DiGit Blot Scanner, LICOR, Bad Homburg, Germany). Final results were normalized with actin levels, expressed as fold change relative to the control group.

2.11 | Statistical Analysis

Statistical analyses were performed using STATGRAPHICS Centurion 18. Version 18.1.12 (Virginia, USA, 2018), and graphics were made using GraphPad Prism 9.0, Version 9.0.0 (121) (GraphPad Software, Inc., San Diego, CA, USA, 2020). Data are expressed as mean ± standard deviation (SD) from independent experiments, each carried out in triplicate. Statistical differences were evaluated by one-way analysis of variance (ANOVA), followed by Tukey's honestly significant difference (HSD) procedure. A p value less than 0.05 was considered statistically significant throughout the analysis. All analyses were performed in triplicate, and the data are presented as mean ± SD.

3 | Results and Discussion

3.1 | Phytochemical Content of Purple Prickly Pear Peel

Prickly pear peel is not considered an edible part of this fruit for humans; however, according to Ada et al. [36], several bioactive compounds are present in higher amounts in the peel compared to the pulp. Therefore, the prickly pear peel by-product could have great potential to be used as starting material for the extraction and production of new bioactive food ingredients. As shown in Table 2 the phytochemical composition of the purple prickly pear peel is characterized by high levels of bioactive compounds, particularly betalains (253.1 ± 13.8 mg BetEq/g DW) and polyphenols (16.50 ± 0.81 mg GAEq/g DW), indicating its potential as a valuable source of functional ingredients.

Regarding betalains, they are the red-violet and yellow-orange pigments that substitute anthocyanins in plants belonging to the Caryophyllales order [37]. Prickly pears are a good source of betalains, which are distributed into two groups, betacyanins and betaxanthins. Betacyanins give the red–purple color, and betaxanthins the yellow–orange, to the fruit. Betanin (betacyanin) and indicaxanthin (betaxanthins) are the most

TABLE 1 | Primer sequences used for quantitative real-time RT-qPCR assay.

Gene	Sequence	
	Forward (5′–3′)	Reverse (5′–3′)
Actin	ACCCACACTGTGCCCATCTA	TCGGTGAGGATCTTCATGAGGTA
BID	CCTTGCTCCGTGATGTCTTTC	TCCGTTCAGTCCATCCCATTT
CASP9	GTCCTACTCTACTTTCCCAGGTTTT	GTGAGCCCACTGCTCAAAGAT
CYCS	TTTGGATCCAATGGGTGATGTTGAG	CCATCCCTACGCATCCTTTA
BCL2	ACCACTAATTGCCAAGCACC	ATTTTCCATCCGTCTGCTCTT
BAX	CCCTTTTGCTTCAGGGTTTC	ACAAAGTAGAAAAGGGCGACAA
CCND1	GAACAAACAGATCATCCGCAA	TGCTCCTGGCAGGCACGGA
CDK4	CTTCCCGTCAGCACAGTTC	GGTCAGCATTTCCAGTAGC
P21	GCGATGGAACTTCGACTTTGT	GGGCTTCCTCTTGGAGAAGAT
PI3K	GAAGCACCTGAATAGGCAAGTCG	GAGCATCCATGAAATCTGGTCGC
mTOR	AGTGGACCAGTGGAAACAGG	TTCAGCGATGTCTTGTGAGG

representative compounds belonging to the betalain family [38]. Betanin represents the most abundant bioactive compound quantified in purple prickly pear peel, 253.1 ± 13.8 mg BetEq/g DW. Similar values were obtained by Smeriglio et al. [39] for samples collected in August 2019 in Messina (Sicily, Italy).

Previous studies have shown that betalains could have a beneficial effect on human health due to their antioxidative, anti-inflammatory, hepatoprotective, and antitumor activities in vitro or in vivo models [40–42]. Regarding the anticancer activity, betalains have been shown to induce apoptosis, reduce cell proliferation, inhibit angiogenesis, and reduce inflammation in animal models and cell lines related to skin, liver, lung, colon, and esophageal cancers [43–45].

Total polyphenol content in peel was way higher than values exposed by Melgar et al. [7] for cactus peel (*O. ficus-indica* var. sanguigna—OS) (3.7 ± 0.3 mg GAeq/g DW) collected in July–August 2016 in Sicily, Italy. Furthermore, the values were higher than the ones reported by Amaya-Cruz et al. [20] in the Roja Lisa variety (9.64 ± 0.50 mg GAEq/g DW) harvested in September 2016 in Guanajuato, Mexico. Additionally, Albergamo et al. [46] reported higher values (47.85 ± 0.73 mg GAEq/g DW) for samples harvested in the coastal area of Mahdia Governorate (northeastern Tunisia) during August 2020.

Additionally, the AsA contents were evaluated, and the concentration was 2.27 ± 0.01 mg/g DW. This value is similar to the one reported by Gómez-Maqueo et al. [47] for red-skinned Sanguinos prickly pears cultivated in Murcia, Spain. Finally, total flavonoid content was also obtained. As it can be observed, the value was low; however, it agrees with some studies reported in literature. For instance, Cardador-Martínez, Jiménez-Martínez, and Sandoval reported a flavonoid concentration of 0.21 mg CatEq/g DW in samples collected in San Luis Potosí, Mexico. In contrast, Amaya-Cruz et al. [20] and Albergamo et al. [46] reported higher values of 2.45 ± 0.29 mg/mL and 29.58 ± 0.30 mg/mL, respectively, compared to those obtained in the present study.

TABLE 2 | Phytochemical composition of purple prickly pear peel.

Bioactive compound	Mean ± SD
Betalains (mg BetEq/g DW)	253.1 ± 13.8
Total polyphenols (mg GAEq/g DW)	16.50 ± 0.81
Ascorbic acid (mg AsA/g DW)	2.27 ± 0.01
Total flavonoids (mg CatEq/g DW)	0.81 ± 0.03

Abbreviation: DW, dry weight.

3.1.1 | Identification and Quantification of Polyphenols

A polyphenols profile depends on several factors, including the plant's genus, species, ripeness, cultivar, growth region, and kind of plant tissue [48]. In the present work, the main phenolic compounds in the extract were detected automatically using a compound extraction algorithm based on the detection of molecular characteristics. The total ion chromatogram (TIC) obtained is shown in Figure S1, and the corresponding peak list is provided in Table S2.

According to the results shown in Table 3, the main two polyphenols quantified were piscidic acid (25.85 ± 1.00 mg/g DW) and eucomic acid (18.50 ± 0.50 mg/g DW). Isorhamnetin and its derivative were quantified in lower amounts.

Regarding piscidic acid, Gómez-Maqueo et al. [47] reported similar results for two varieties of *O. ficus-indica* L. Mill (purple and red) with 51.9 ± 0.34 mg/g DW and 29.3 ± 0.06 mg/g DW, respectively. Eucomic acid was quantified by Melgar et al. [7] in red peel from fruits collected in July–August 2016 in Sicily, Italy; the value was lower (2.2 ± 0.2 mg/g DW) compared with the results obtained in this work. Dihydroferulic acid glucuronide has been quantified in the methanolic extract of green peel from *Opuntia leucotricha* DC [49]; however, to our knowledge, this has been the first time that it is detected in *O. ficus-indica*. Other phenolic acids were detected in low concentrations, including protocatechuic acid glucoside, ferulic acid glucoside, and methyl-eucomic acid.

Several flavonoids have been reported in *O. ficus-indica* peel and pulp, and one of the most abundant is isorhamnetin and its derivative, which are mainly found in the form of at least five different di- and triglycosides [50]. In this study, isorhamnetin and its derivatives constitute the main flavonoid detected, but

TABLE 3 | Mass spectral data, retention time, and concentration of compounds tentatively identified in the extract of purple prickly pear peel (PPP), expressed as mg of compound/g of PPP.

Proposed compound	$[M-H]^-$ m/z	Retention time (min)	Concentration (mg/g of PPP *DW)
Phenolic acids			
Methyl-eucomic acid	253.0575	2.86	0.17 ± 0.00
Protocatechuic acid glucoside	315.0726	8.67	0.16 ± 0.00
Piscidic acid isomer 1	255.0514	9.17	25.00 ± 1.00
Piscidic acid isomer 2	255.0511	10.67	0.85 ± 0.01
Eucomic acid	239.0566	12.61	18.50 ± 0.50
Ferulic acid glucoside	355.1038	13.14	0.60 ± 0.10
Dihydroferulic acid glucuronide	371.0988	15.95	0.41 ± 0.01
Flavonoids			
Isorhamnetin-rutinoside-rhamnoside isomer 1	769.2194	16.78	0.50 ± 0.00
Isorhamnetin-rutinoside-rhamnoside isomer 2	769.2199	17.2	0.23 ± 0.00
Kaempferol 3-O-glucosyl-rhamnosyl-glucoside	755.204	17.31	0.85 ± 0.01
Quercetin neohesperidoside	609.1463	19.31	0.37 ± 0.00
Isorhamnetin-neohesperoside	623.1617	21.12	0.82 ± 0.01
Isorhamnetin	315.0509	33.26	0.19 ± 0.01

*DW: dry weight.

also quercetin and kaempferol have been identified. Previous studies have demonstrated similar composition [15, 51].

During the investigation about the beneficial effect of the main polyphenols present in the extract analyzed in this study, it was found that ferulic acid and ferulic acid derivatives possess anti-inflammatory, antiproliferative, proapoptotic, antiangiogenic, and/or antimetastatic effects against lung, colorectal, liver, breast, cervical, osteosarcoma, and glioblastoma cancer [52]. The most abundant polyphenol in the extract, piscidic acid, is linked to high antioxidant capacity and anti-inflammatory and anti-adipogenic effects [53]. Hernández et al. [54] reported piscidic acid as the most abundant polyphenol in prickly pear fruits. Interestingly, the presence of piscidic acid in nature is not very common; it is mainly associated with succulent plants with crassulacean acid metabolism (CAM) [23]. On the other hand, eucomic acid is another important phenolic acid in the Cactaceae family [55], and it is also a good antioxidant. This phenolic acid has been shown to protect skin cells from UV radiation, against UV-induced apoptosis, and to reduce inflammation in adipocytes [56]. Finally, isorhamnetin and its derivatives have extensive biological activities. These flavonoids are related to modulating key signaling pathways, including PI3K/AKT, MAPK, p53, NF-κB, and EMT. For that reason, they have been widely investigated in experimental cancer-related studies [57].

3.2 | Total Antioxidant Capacity of Purple Prickly Pear Peel

The antioxidant and free-radical scavenging properties of the purple prickly pear peel were investigated by several in vitro assays (Table 4). The extract exhibited a reducing capacity of 23.25 ± 0.54 μmol Txeq/g DM through the FRAP method, indicating a substantial antioxidant potential. This value was similar to the one obtained by Smeriglio et al. [32], which was 19.54 ± 0.63 μmol Txeq/g DW.

TABLE 4 | Total antioxidant capacity of purple prickly pear peel (μmol Txeq/g DW).

Method	Value
FRAP	23.25 ± 0.54
DPPH	17.19 ± 0.68
TEAC	22.14 ± 0.09
ORAC	83.20 ± 3.0

Abbreviations: DW, dry weight; Txeq, Trolox equivalent.

DPPH, TEAC, and ORAC methods also showed that the peel has antiradical potential: the values for the radical quenching capacity equivalent were 17.19 ± 0.68, 22.14 ± 0.09, and 83.20 ± 3.0 μmol Txeq/g DW, respectively. These results suggest that PPE has a moderate to high capacity to donate electrons or hydrogen atoms to neutralize free radicals, thereby contributing to its overall antioxidant profile, and a higher value is shown with the ORAC assay. Similar results were obtained by Smeriglio et al. [32] and Gómez-Maqueo et al. [47]. Taking all of these together, these values suggest that PPE possesses notable antioxidant properties, although the magnitude of the effect depends on the assay employed.

3.3 | Tumorigenic Cancer Cells' Viability Was Negatively Affected by PPE

To evaluate the effect of PPE on the proliferation of the cancer cell line (HCT116) and the nontumorigenic cell line (CCD-18c), the MTT assay was used. In this study, cells were treated with increasing concentrations of PPE, ranging from 0 to 15 mg/mL, to figure out whether the effect could be dose-time dependent. Finally, SI was also obtained to examine whether the extract possesses selective toxicity against cancer cells. As expected, the extract significantly reduced the proliferation of HCT116 cells in a dose- and time-dependent manner (Figure 1a), attributable to

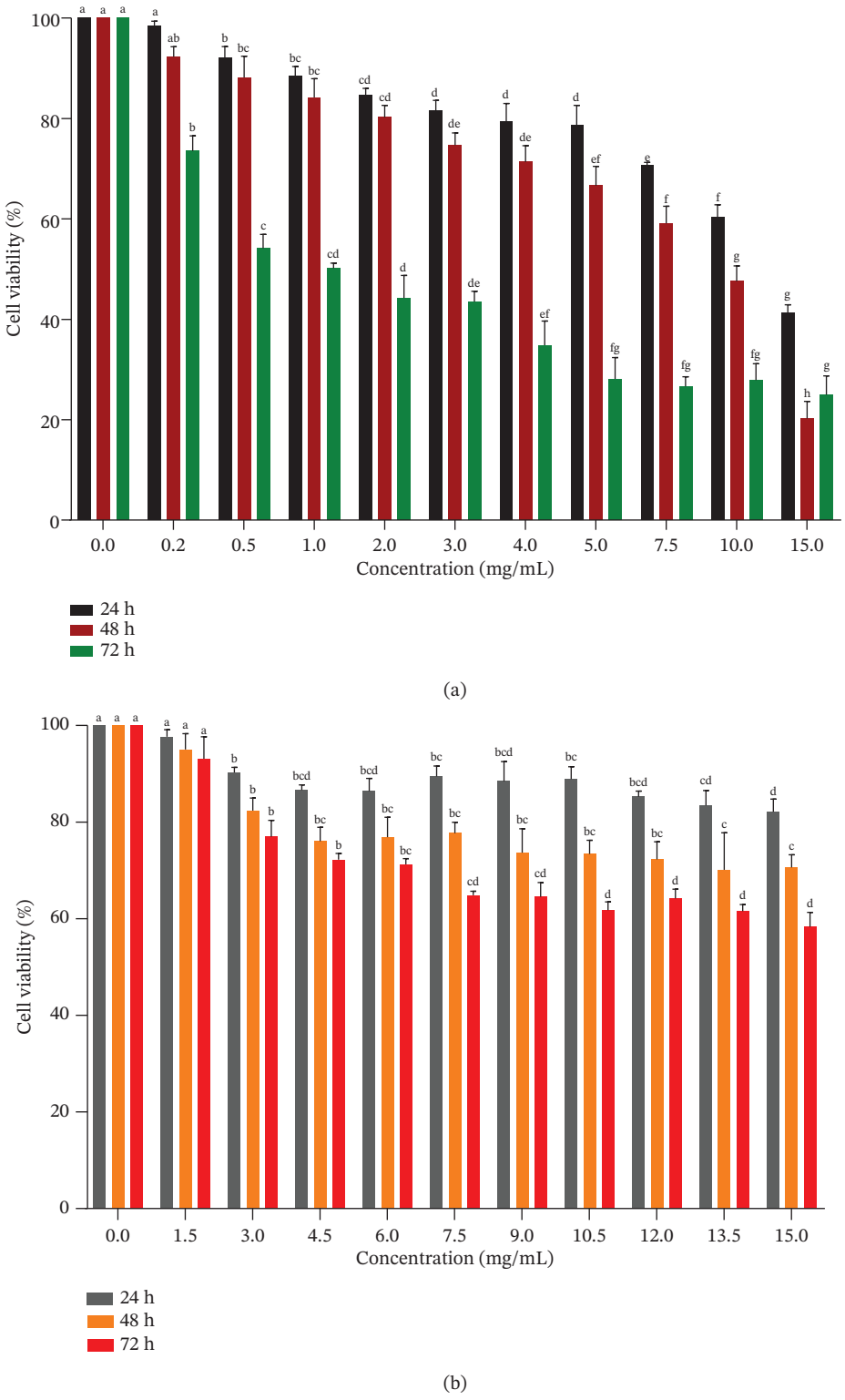

FIGURE 1 | Effect of PPE extract on proliferation of tumorigenic cells (HCT116) and nontumorigenic cells (CCD-18c). After treatment times of 24, 48, and 72 h, cell viability was estimated by MTT assay, and the results were expressed as % of viable (a) HCT116 and (b) CCD-18c cell lines with respect to the control (untreated cells). Mean values and their standard deviations are reported ($n = 3$).

the high content of bioactive compounds present in PPE. The IC_{30}, IC_{50}, and IC_{70} obtained were 4.65, 8.91, and 12.68 mg/mL, respectively..

The same concentration range was used to evaluate the effect on nontumorigenic cells. As is shown in Figure 1b, the extract possesses less cytotoxicity for nonmalignant cells compared to cancer cells, with IC_{30}, IC_{50}, and IC_{70} values of 12.6, 24.1, and 35.6 mg/mL, respectively. This behavior is a key point for anticancer extract development. Selective Index values ranged from 2.7 to 2.8, suggesting that PPE possesses particular effectiveness against tumorigenic cells, with lower impact on noncancerous

cells [34] due to the SI being higher than 2 in all cases. However, the SI magnitude was not very high, indicating that the selectivity was not very strong, but at the same time, it was observed that for nontumorigenic cells, the viability remains around 70% even after 72 h of treatment, whereas for tumor cells, it decreased up to 20%, indicating that PPE has a stronger effect on tumor cells.

Despite differences in experimental protocols, El-Beltagi et al. [58] also showed that peel cactus extract effectively inhibited the growth of cancer cells in a dose-dependent manner. In that case, the cancer cell lines tested were liver cell line (HepG2), colorectal adenocarcinoma (Caco-2), and breast cell line (MCF-7). A similar effect was observed by Ali et al. [59] in breast cancer (MCF-7 and MDA-MB-231 cell lines) and HepG2 cancer cell lines by Önem et al. [60]. Further experiments were conducted to delve into the molecular mechanisms underlying the role of PPE in HCT 116 cell line cell-growth inhibition. For this purpose, PPE concentrations of 4.0, 8.0, and 12.0 mg/mL were used according to the IC_{30}, IC_{50}, and IC_{70} obtained here. In addition, betanin (5 mM) was evaluated as a positive control due to the literature where the authors agree that this is the main bioactive compound present in purple prickly pear peel [39]. The betanin concentration chosen represented, approximately, the equivalent of betanin in a concentration of 8.0 mg of extract/mL.

3.4 | Purple Prickly PPE Promotes Cell Apoptosis in HCT116 Cells

Given the fact that apoptosis induction is one of the main mechanisms used by polyphenols or bioactive compounds in general to release their effect against cancer development and progression [61], a Tali™ Image-Based Cytometer analysis was first conducted with double-staining of Annexin V–Alexa Fluor® 488 and PI to evaluate the possible apoptosis activation by PPE in the HCT116 cell line. The results, observed in Figure 2, show that PPE treatment has significantly ($p < 0.05$) increased apoptotic population cells in a dose-dependent manner, specifically early apoptotic cells (Figure 2a, green bars). The proportion of apoptotic cells reached values up to 3.33-fold compared to untreated cells. These findings suggest that PPE induced apoptosis in HCT116 cells, with a remarkable apoptotic response at higher concentrations.

Between the different mechanisms for programmed cell death, apoptosis is considered the most common [62]. During the development of CRC, the balance between cell growth and apoptosis rates that keep intestinal epithelial cell homeostasis gets progressively unbalanced. Previous studies have highlighted the possible strong connection between failed apoptosis and the progression of CRC and its poor response to chemotherapy and radiation [63–66]. To support the potential pro-apoptotic effect of prickly pear, Zou et al. [67] showed that aqueous extracts of prickly pear induced apoptosis in ovarian, cervical, and bladder cancer cells, with the strongest effect found in cervical cells. In addition, Caco-2 cells were in early apoptosis after treatment with aqueous extract of prickly pear (yellow cultivar) [68].

3.5 | Purple Prickly PPE Induces Intrinsic Apoptotic Pathway Through p53 Activation

To gain mechanistic insight into the apoptosis induction by PPE in HCT116 cells, several key apoptotic markers were measured through RT-qPCR and Western blot. First of all, the effect of PPE on the protein expression of the tumor suppressor protein, p53, was assessed. p53 regulates many genes involved in cell apoptosis due to its role as a nuclear transcription factor, which is activated after various stresses, such as DNA damage, oncogene expression, and oxidative stress [69]. As can be observed in Figure 3, the treatment significantly ($p < 0.05$) upregulated the expression of p53 at protein levels. This result is consistent with the previous report by Feugang et al. [70], which showed that a cactus pear mixture aqueous extract (CME) increased the levels of DNA fragmentation, together with the upregulation of several proteins, including p53.

Due to its preventive and inhibiting role in cancer progression, p53 is called the 'guardian of the genome' [71]. In response to cellular stress, such as DNA damage, intracellular p53 protein levels are increased, and it binds to target DNA; as a consequence, it regulates the transcription of various genes involved in apoptosis, including Puma, Bax, and Noxa [72, 73]. Based on the previous explanation, the effect of p53 overexpression was explored in the transcription of several genes involved in the intrinsic apoptotic pathway by using RT-qPCR. The results, presented in Figure 4, showed that the treatment significantly ($p < 0.05$) upregulated the expression of several pro-apoptotic genes, such as BAX, BID, CASP9, and CYCS, as indicated by the fold-change increase up to 1.87, 3.14, 1.52, and 1.89, respectively. Conversely, BCL2 was significantly ($p < 0.05$) downregulated up to a 0.47-fold change relative to control after treatment.

These findings suggest that p53 could transcriptionally activate the expression of pro-apoptotic BCL-2 family genes, such as BID and BAX, whereas it inactivates the expression of anti-apoptotic BCL-2, leading to mitochondrial apoptosis induction. This hypothesis is also linked to the overexpression of CASP9 and CYCS obtained after treatment. Even though scarce information is available regarding p53 activation by prickly pear, according to Abid et al. [74], *Opuntia monocantha* ethanolic extract induced apoptosis in HepG2 cells via a p53-dependent pathway. In addition, cactus pear CME significantly increased the population of apoptotic ovarian cancer cells, and it was linked to the upregulation of BAX and CASP3 at gene levels [70].

3.6 | Purple Prickly PPE Induced Cell Cycle Arrest at the Sub-G1 Phase

The cell cycle is the process by which an original cell is divided to give rise to two genetically identical cells [75]. Monitoring DNA damage during all four phases of the cell cycle is a key point to ensure the proper proliferation, growth, and survival of cells [76]. This approach is used by several cell cycle agents, including plant extracts, to interfere with the cell cycle and stop cancer cells at specific phases of the cycle [77]. To evaluate whether PPE had some effect on cell cycle arrest, the Tali™ Cell Cycle Kit was used by staining with PI and using the Tali Image-Based Cytometer. After 48 h of treatment, a significant ($p < 0.05$) increase of cells at the sub-G1 phase was observed (Figure 5). The lowest treatment (4 mg/mL) did not increase significantly with respect to the control, but the highest concentration (12 mg/mL) increased the cells in the sub-G1 phase up to 38%. In literature, it is established that the sub-G1 phase indicates DNA fragmentation, which occurs in the late stage of apoptosis [78]; however, the sub-G1 results should always be together with other assays to confirm the presence of apoptosis [62]. Due to the results shown

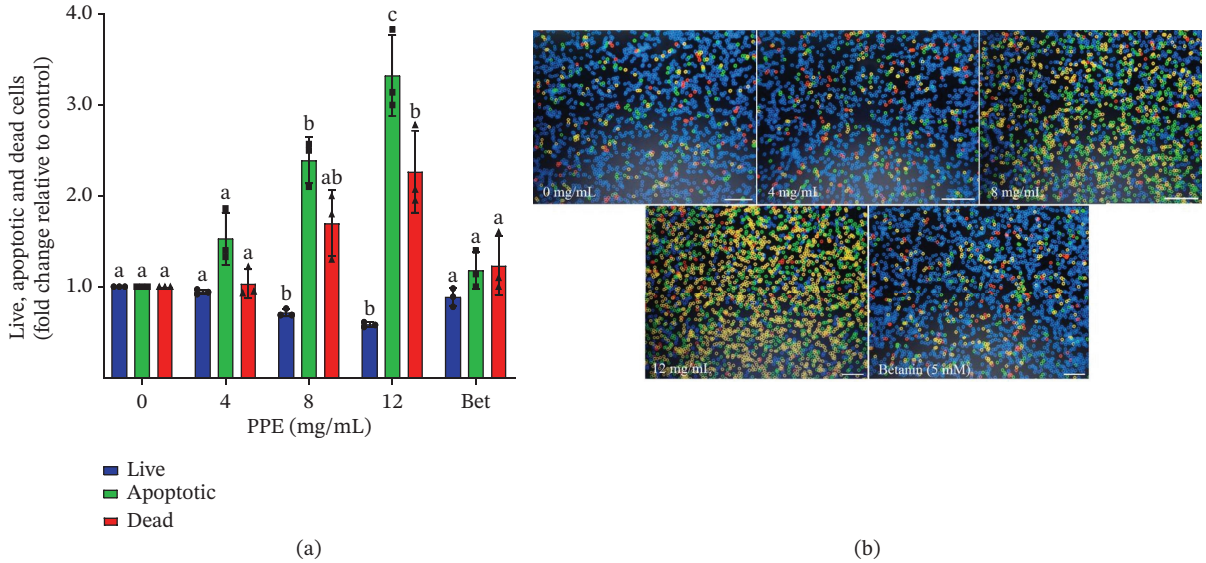

(a) (b)

FIGURE 2 | PPE induced apoptosis in the HCT116 cell line. Cells were treated with 4, 8, and 12 mg/mL of PPE, betanin (Bet, 5 mM), and media (0 mg/mL) for 48 h. (a) Percentage of Annexin V Alexa Fluor® 488/PI double-stained HCT 116 cells was determined by the Tali™ image-based cytometer compared to the control group (0 mg/mL). (b) Representative Tali™ image-based cytometer images: blue color corresponds to live cells, green color corresponds to early apoptotic cells, and yellow and red colors correspond to late apoptotic and dead cells, respectively. Scale bar = 200 μm. Mean values and their standard deviations are reported ($n = 3$). Different superscript letters for each column indicated significant differences ($p < 0.05$).

previously (3.2), it can be highlighted that the changes induced in cells during cell cycle progression align with its apoptotic effects, which confirm the pro-apoptotic ability of PPE on HCT116 cells.

According to Serra et al. [79], polyphenol-rich concentrates from *O. ficus-indica* and *Opuntia robusta* fruit juices induced cell cycle arrest at different checkpoints of human colon cancer cells (HT-29), and the effect was ascribed mainly to betacyanins, isorhamnetin derivatives, and phenolic acids such as piscidic and ferulic acid present in the extracts.

3.7 | Purple Prickly PPE Dysregulates Cell Cycle-Related Gene Levels

Having observed that PPE induced cell cycle arrest at the sub-G1 phase, the mRNA expression of several cell cycle arrest markers at the G1 phase was determined in HCT116. Regarding this, in Figure 6 following the treatment, P21 was significantly ($p < 0.05$) upregulated, meanwhile CDK4 and its regulatory subunit, CCND1 were significantly ($p < 0.05$) downregulated. Specifically, P21 increased its expression from 1.13 to 1.93-fold, CDK4

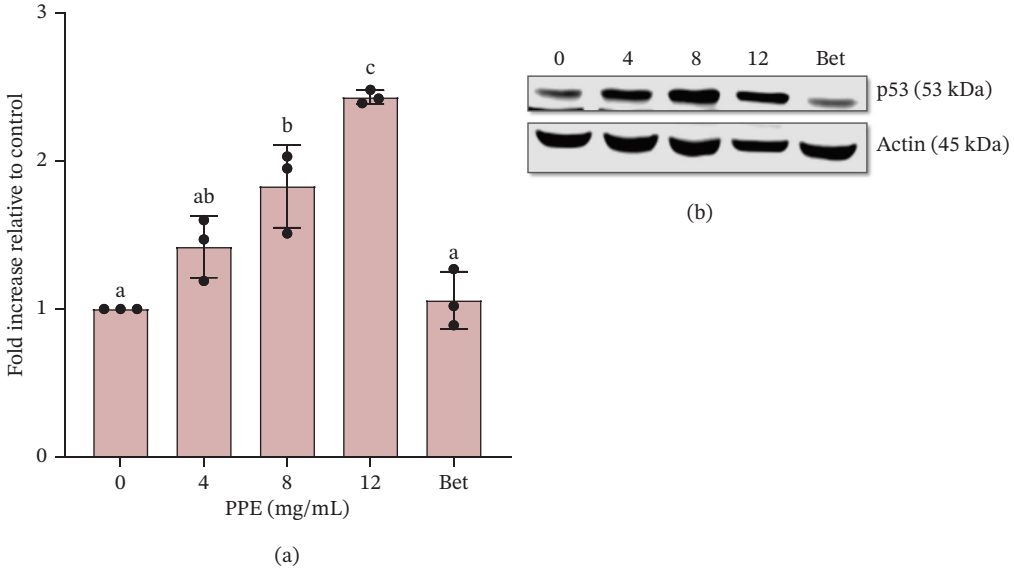

(a) (b)

FIGURE 3 | PPE upregulated the protein expression of the tumor suppressor protein, p53. Cells were treated with increasing concentrations of PPE (4, 8, and 12 mg/mL) and betanin (Bet, 5 mM) for 48 h. Protein expression of apoptotic markers, p53, is shown in (a) a graphic quantitative Western blot analysis normalized for actin and (b) a representative image of the fluorescent signal. Error bars represent the standard deviation (SD) from the average of three, separate experiments ($n = 3$). The statistical difference ($p < 0.05$) between each level of protein load is shown by letters. The original uncropped Western blot images are provided in Figures S2 and S3.

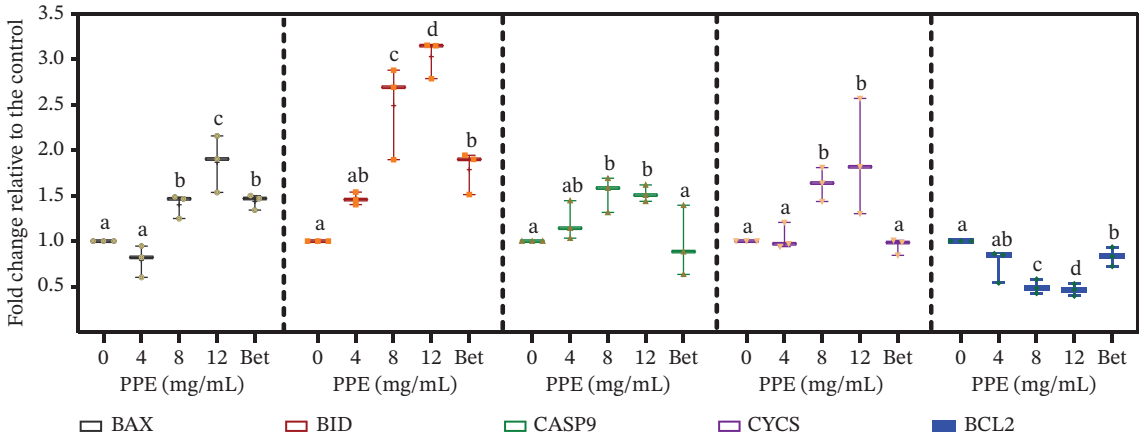

FIGURE 4 | PPE treatment modulated the mRNA expression of several genes implicated in the intrinsic apoptotic pathway. Cells were exposed to increasing concentrations of PPE (4, 8, and 12 mg/mL) and betanin (Bet, 5 mM) for 48 h. BAX, BID, CASP9, CYCS, and BCL2 marker mRNA expression were analyzed using RT-qPCR, and actin was used to normalize the results. Data are presented as the mean ± SD ($n = 3$ independent samples). Statistical significance ($p < 0.05$) was assessed using different letters.

reduced its expression from 1.04 to 0.30-fold, and CCND1 from 0.83 to 0.63-fold.

P21 is well-known for inhibiting the cell cycle and arresting the cell cycle progression in G1/S and G2/M transitions by inhibiting CDK4,6/cyclin-D and CDK2/cyclin-E complexes, respectively [80]. P21 is strongly induced by p53. In this sense, p53 binds to one part in the p21/CDNKN1A promoter and activates its transcription [81]. As found previously in this study, PPE upregulated the expression of p53 at protein levels so the overexpression of P21 could be p53-dependent.

Based on these results, it can be speculated that following DNA damage due to the pro-oxidant effect of PPE, p53 expression is induced and as a consequence triggers intrinsic apoptosis and cell cycle arrest through p21 upregulation in CRC cells.

3.8 | Purple Prickly PPE Triggers ROS Generation in HCT116 Cells

ROS act as a double-edged sword in cancer because at low to moderate concentrations they activate several proto-oncogenes and inactivate some tumor suppressor genes and, as a result,

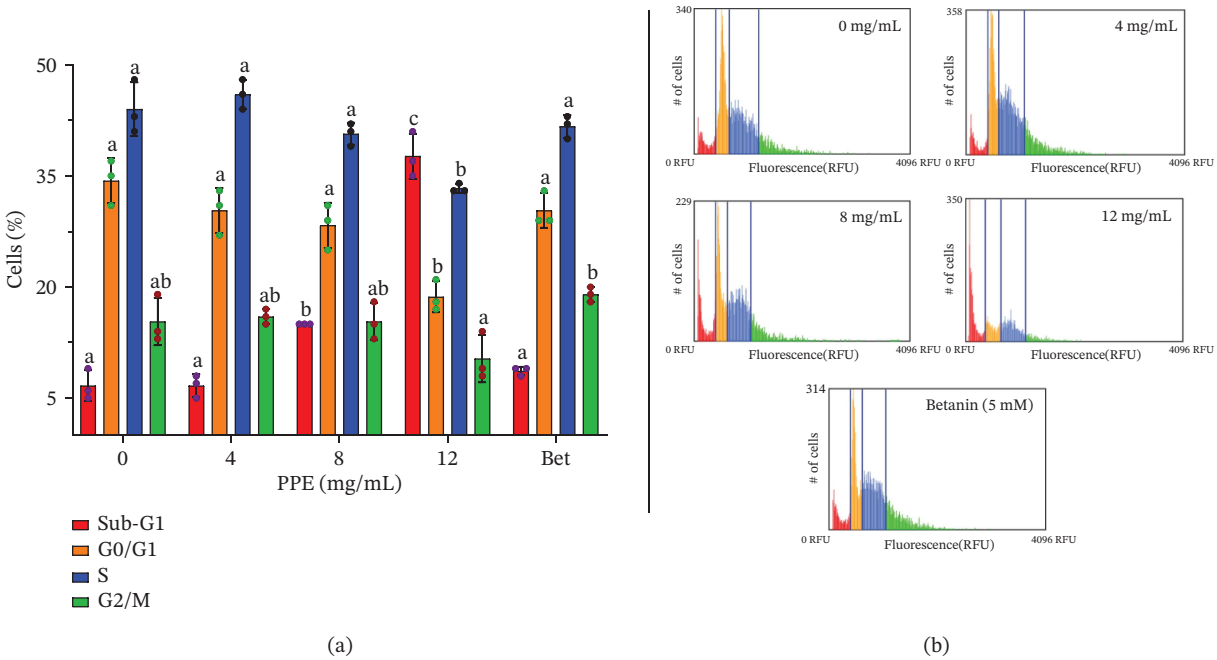

FIGURE 5 | PPE modulates the cell cycle in the HCT116 cell line. Cells were treated for 48 h as described in the methods section. After treatment, cells were collected and analyzed by the Tali™ image-based cytometer. (a) Histograms represent quantitative analysis of cell distribution in the cell cycle progression, and (b) representative images after the Tali™ image-based cytometer assay: red color represents the sub-G1 phase, orange color the G0/G1 phase, blue color the S phase, and green color the G2/M phase. Data are presented as the mean ± SD ($n = 3$ independent samples). Statistical significance ($p < 0.05$) was assessed using different letters.

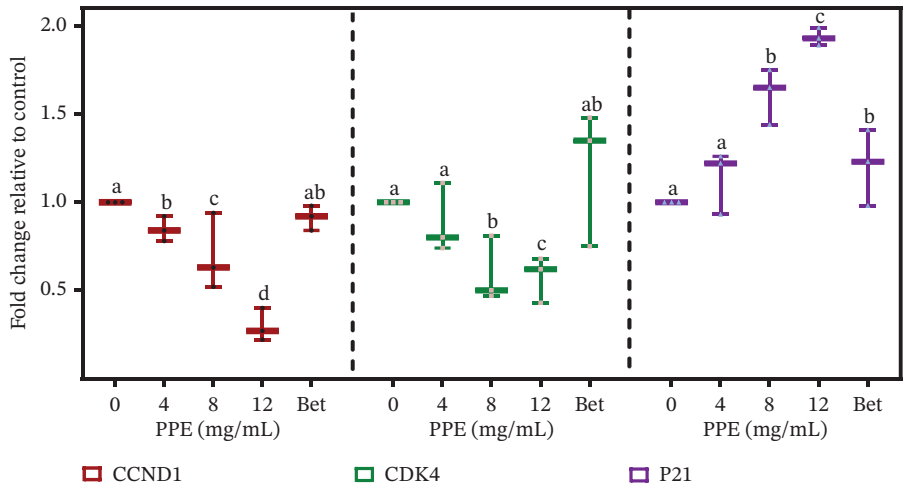

FIGURE 6 | PPE treatment modulated the mRNA expression of several key regulatory genes related to the cell cycle progression. Cells were cultivated for 48 h as described in the methods section. The mRNA expressions of CCND1, CDK4, and P21 markers were evaluated using RT-qPCR. Data are presented as the mean ± SD ($n = 3$ independent samples). Statistical significance ($p < 0.05$) was assessed using different letters.

induce abnormal cell growth and metastasis. In contrast, when the ROS levels exceed the tipping point, antitumor effects are stronger via the induction of apoptosis and cell cycle arrest [82, 83]. In this regard, plenty of studies have emphasized the potential of plant extracts as antineoplastic agents, possibly because their pro-oxidant constituents can enhance intracellular ROS production [84]. Following this statement, the anti-proliferative and proapoptotic effect of PPE was investigated, highlighting if it could be linked to increasing the intracellular ROS generation by using the CellROX® oxidative stress kit. As expected, PPE treatment significantly ($p < 0.05$) increased the ROS generation in HCT116 (Figure 7). The highest concentration upregulated the intracellular ROS generation, up to a 3.0-fold increase compared to untreated cells.

Previous studies have highlighted the significant effect of prickly pear on intracellular ROS generation. For instance, cactus pear CME treatment significantly increased the ROS accumulation in ovarian cancer cells, but the induction in immortalized ovarian epithelial was only slight at high concentrations [70]. Furthermore, in the colorectal adenocarcinoma cell line (HT-29), *Opuntia* spp. extract promoted an increase in ROS production with respect to the control [79].

Based on the fact that in our study, ROS levels increased in treated cells compared with untreated cells, we speculate that ROS could be the driving point for apoptosis induction and cell cycle arrest in HCT116 after being treated with different concentrations of PPE.

3.9 | Proliferation of HCT-116 Cells Was Negatively Affected by Purple Prickly PPE

To support the potential antiproliferative effect of PPE in HCT116 cells, additional experiments were conducted regarding the effect on EGFR and PI3K/AKT/mTOR pathways. HER2

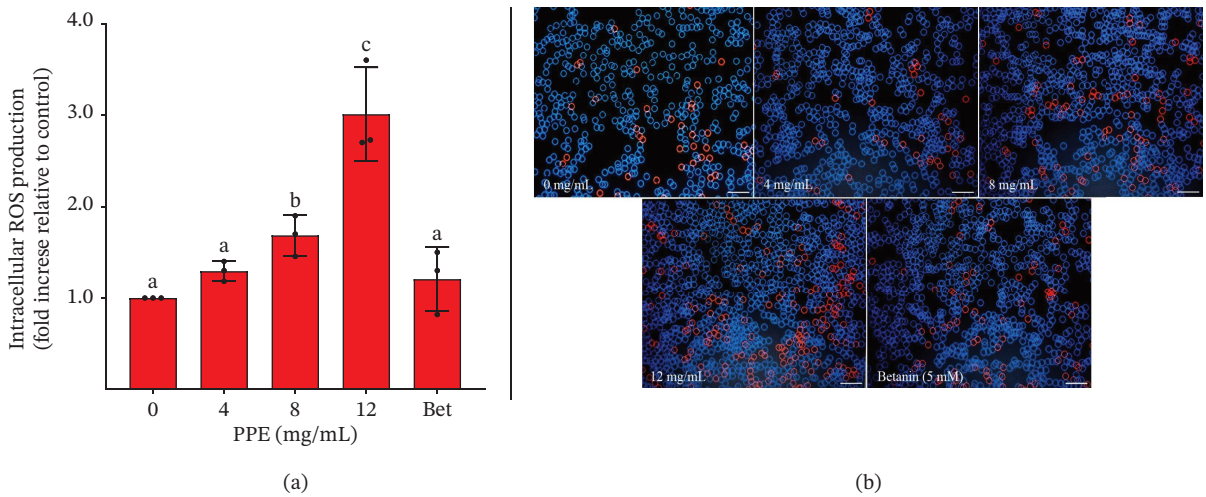

(a) (b)

FIGURE 7 | Effect of PPE in intracellular ROS production in HCT 116 cells. Cells were cultivated for 48 h and treated as described in the methods section. After treatment, cells were harvested, stained using the CellROX® Orange assay kit, and processed by the Tali™ image-based cytometer. (a) Histograms represent quantitative analysis of intracellular ROS levels, and (b) representative images after the Tali™ image-based cytometer assay: red circles represent ROS-induced cells. Scale bar = 200 μm. Data are compared to untreated cells (0 mg/mL), and they are presented as the mean ± SD ($n = 3$). Statistical significance ($p < 0.05$) was assessed using different letters.

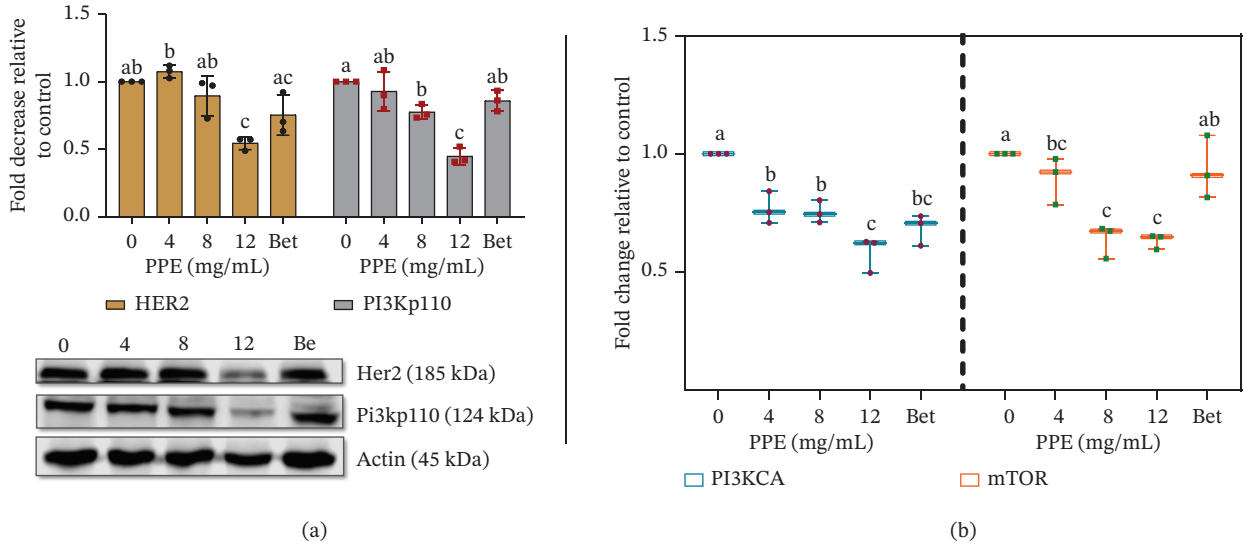

(a) (b)

FIGURE 8 | PPE treatment affects at gene and protein levels several key regulatory proteins regarding the EGFR signaling pathway. Cells were treated with increasing concentrations of PPE (4, 8, and 12 mg/mL) and betanin (Bet, 5 mM) for 48 h. After treatments, cells were collected, and (a) mRNA expression of PI3KCA and mTOR was analyzed using RT-qPCR and (b) protein levels of HER2 and PI3K were quantitatively analyzed by Western blot, normalized for actin, and a representative graphic and image of the fluorescent signal were observed. All data shown are the mean ± SD ($n = 3$). Different letters within each column indicate significant differences between treatments ($p < 0.05$). The original uncropped Western blot images are provided in Figures S4–S7.

belongs to the EGFR family; its phosphorylation by several ligands can activate downstream signaling pathways, including the PI3K/AKT/mammalian target of rapamycin (mTOR) [85]. The activation of these pathways is connected directly with multiple pathways in cancer development, including various aspects of cell growth, tumor progression, survival, metabolism, apoptosis, and cell death [86, 87].

In the present study, the expressions of Her2 and PI3K were analyzed at protein levels; PI3K was also analyzed at mRNA levels together with mTOR in HCT116 cells. After the treatment, a notable decrease in Her2 protein expression (Figure 8a) was observed in comparison to untreated cells. Her2 expression decreased up to 0.56-fold, but in this case, at 4 mg/mL, the value slightly increased up to 1.15. Regarding the EGFR downstream signaling, gene expressions of PI3KCA and mTOR decreased significantly ($p < 0.05$) (Figure 8b) in a dose-dependent manner (expression decreased up to 0.58 and 0.63-fold, respectively, compared to the control). In the case of PI3K, the decreased effect was also observed at protein levels (Figure 8a); in this case, the values reduced up to 0.45-fold relative to untreated cells. These observations may suggest that PPE's antiproliferative effect could be linked to the downregulation of EGFR and PI3K/AKT/mTOR pathways.

Numerous investigations indicate that betalain, specifically betanin, could be considered a strong chemopreventive compound due to its effect against proliferation, angiogenesis, and inflammation in skin, liver, lung, colon, and esophageal cancers in experimental animals and cancer cell lines, together with its proapoptotic action [45]. Interestingly, in this study, the betanin standard at 5 mM did not induce any significant or clear change in the proliferation and apoptosis in the HCT116 cell line. The parameters evaluated in this work showed scarce or random effects of betalin (5 mM) against HCT116 proliferation. Therefore, it could be speculated that the effect of prickly PPE is likely linked to a synergistic effect of its bioactive compounds rather than to individual constituents.

4 | Conclusions

In conclusion, this study demonstrates that purple prickly pear peel exhibits potent antiproliferative and proapoptotic effects against human CRC cells, mediated through apoptosis induction and ROS generation, cell cycle arrest, and modulation of some molecules involved in EGFR and PI3K/AKT/mTOR pathways. Considering the results obtained in this work, developing effective strategies to valorize prickly pear peel waste can be considered a source of products that could have a high value, despite previously being a waste product; therefore, it would reduce environmental waste. These findings highlight the potential use of discarded prickly pear peel as a valuable source of bioactive compounds with promising applications as nutraceutical or functional ingredients. It is important to point out that additional studies are required to evaluate the bioavailability and bioaccessibility of bioactive compounds, along with in vivo and clinical studies. Nevertheless, it should be considered that this study represents a starting point for obtaining preliminary data for further studies, and there is very little scientific information that validates the positive effect of prickly pear peel on human health.

Acknowledgments

The authors are grateful to Consorzio Euroagrumi O.P. Biancavilla for kindly and generously supporting the provision of the purple prickly pear used in this research.

Funding

This research did not receive any specific grant from funding agencies in the public, commercial, or not-for-profit sectors.

Conflicts of Interest

The authors declare no conflicts of interest.

Data Availability Statement

Data are available on request from the authors.

References

1. G. Roshandel, F. Ghasemi-Kebria, and R. Malekzadeh, "Colorectal Cancer: Epidemiology, Risk Factors, and Prevention," *Cancers* 16, no. 8 (2024): 1530, https://doi.org/10.3390/cancers16081530.

2. Y. Huang, W. Hong, and X. Wei, "The Molecular Mechanisms and Therapeutic Strategies of Emt in Tumor Progression and Metastasis," *Journal of Hematology & Oncology* 15, no. 1 (2022): 129, [In eng], https://doi.org/10.1186/s13045-022-01347-8.

3. M. G. Cerrito and E. Grassilli, "Identifying Novel Actionable Targets in Colon Cancer," *Biomedicines* 9, no. 5 (2021): 579, https://doi.org/10.3390/biomedicines9050579.

4. J. Wu, Y. Li, Q. He, and X. Yang, "Exploration of the Use of Natural Compounds in Combination With Chemotherapy Drugs for Tumor Treatment," *Molecules* 28, no. 3 (2023): 1022, [In eng], https://doi.org/10.3390/molecules28031022.

5. F. Shiridokht, P. Kehtari, M. Eskandani, A. Farajollahi, and S. Vandghanooni, "Advancing Cancer Radiotherapy: Harnessing Radiosensitizers and Nanotechnology for Enhanced Tumor Control," *International Journal of Pharmaceutics* 10 (2025): 100419, https://doi.org/10.1016/j.ijpx.2025.100419.

6. M. Rudrapal, S. J. Khairnar, J. Khan, et al., "Dietary Polyphenols and Their Role in Oxidative Stress-Induced Human Diseases: Insights into Protective Effects, Antioxidant Potentials and Mechanism(S) of Action," *Frontiers in Pharmacology* 13 (2022): 806470, [In English]. Review, https://doi.org/10.3389/fphar.2022.806470.

7. B. Melgar, M. I. Dias, A. Ciric, et al., "By-Product Recovery of Opuntia Spp. Peels: Betalainic and Phenolic Profiles and Bioactive Properties," *Industrial Crops and Products* 107 (2017): 353–359, https://doi.org/10.1016/j.indcrop.2017.06.011.

8. W. Zeghbib, F. Boudjouan, V. Vasconcelos, and G. Lopes, "Phenolic Compounds' Occurrence in Opuntia Species and Their Role in the Inflammatory Process: A Review," *Molecules* 27, no. 15 (2022): 4763, [In eng], https://doi.org/10.3390/molecules27154763.

9. A. Alibakhshi, R. Malekzadeh, S. Azimeh Hosseini, and H. Yaghoobi, "Investigation of the Therapeutic Role of Native Plant Compounds Against Colorectal Cancer Based on System Biology and Virtual Screening," *Scientific Reports* 13, no. 1 (2023): 11451, https://doi.org/10.1038/s41598-023-38134-5.

10. F. Giampieri, D. Cianciosi, J. M. Alvarez-Suarez, et al., "Anthocyanins: What Do We Know Until Now?" *Journal of Berry Research* 13, no. 1 (2023): 1–6, https://doi.org/10.3233/jbr-220087.

11. D. Cianciosi, T. Forbes-Hernandez, Y. A. Diaz, et al., "Manuka Honey's Anti-Metastatic Impact on Colon Cancer Stem-Like Cells: Unveiling Its Effects on Epithelial–Mesenchymal Transition, Angiogenesis and Telomere Length," *Food & Function* 15, no. 13 (2024): 7200–7213, https://doi.org/10.1039/D4FO00943F.

12. K. El-Mostafa, Y. El Kharrassi, A. Badreddine, et al., "Nopal Cactus (Opuntia Ficus-Indica) as a Source of Bioactive Compounds for Nutrition, Health and Disease," *Molecules* 19, no. 9 (2014): 14879–14901, [In eng], https://doi.org/10.3390/molecules190914879.

13. M. Kaur, A. Kaur, and R. Sharma, "Pharmacological Actions of Opuntia Ficus Indica: A Review Article," *Journal of Applied Pharmaceutical Science* 2, no. 7 (2012): 15–18, https://doi.org/10.7324/JAPS.2012.2703.

14. A. P. Louppis, M. S. Constantinou, I. S. Kosma, A. V. Badeka, F. Blando, and M. G. Kontominas, "Botanical Differentiation of Italian Prickly Pear Varieties: Unveiling Unique Profiles Through Physicochemical Parameters, Volatiles, Antioxidants, and Vitamins," *Microchemical Journal* 214 (2025): 113897, https://doi.org/10.1016/j.microc.2025.113897.

15. A. Diaz, Yasmany, M. Machì, et al., "Prickly Pear Fruits From Opuntia Ficus-Indica Varieties as a Source of Potential Bioactive Compounds in the Mediterranean Diet," *Mediterranean Journal of Nutrition and Metabolism* 15, no. 4 (2022): 581–592, https://doi.org/10.3233/mnm-220102.

16. M. Martins, M. H. Ribeiro, and C. M. M. Almeida, "Physicochemical, Nutritional, and Medicinal Properties of Opuntia Ficus-Indica (L.) Mill. and Its Main Agro-Industrial Use: A Review," *Plants* 12, no. 7 (2023): 1512, https://doi.org/10.3390/plants12071512.

17. A. Mata, J. P. Ferreira, C. Semedo, T. Serra, C. M. Duarte, and M. R. Bronze, "Contribution to the Characterization of Opuntia Spp. Juices by Lc-Dad-Esi-Ms/Ms," *Food Chemistry* 210 (2016): 558–565, [In eng], https://doi.org/10.1016/j.foodchem.2016.04.033.

18. C. E. Aruwa, S. Amoo, and T. Kudanga, "Phenolic Compound Profile and Biological Activities of Southern African Opuntia Ficus-Indica Fruit Pulp and Peels," *Lebensmittel-Wissenschaft und-Technologie* 111 (2019): 337–344, https://doi.org/10.1016/j.lwt.2019.05.028.

19. M. De Wit, A. DuToit, G. Osthoff, and A. Hugo, "Antioxidant Content, Capacity and Retention in Fresh and Processed Cactus Pear (Opuntia Ficus-Indica and O. robusta) Fruit Peels From Different Fruit-Colored Cultivars," *Frontiers in Sustainable Food Systems* 4 (2020): 133, [In English], https://doi.org/10.3389/fsufs.2020.00133.

20. D. M. Amaya-Cruz, I. F. Pérez-Ramírez, J. Delgado-García, C. Mondragón-Jacobo, A. Dector-Espinoza, and R. Reynoso-Camacho, "An Integral Profile of Bioactive Compounds and Functional Properties of Prickly Pear (Opuntia Ficus indica L.) Peel With Different Tonalities," *Food Chemistry* 278 (2019): 568–578, https://doi.org/10.1016/j.foodchem.2018.11.031.

21. R. Gheribi, Y. Habibi, and K. Khwaldia, "Prickly Pear Peels as a Valuable Resource of Added-Value Polysaccharide: Study of Structural, Functional and Film Forming Properties," *International Journal of Biological Macromolecules* 126 (2019): 238–245, https://doi.org/10.1016/j.ijbiomac.2018.12.228.

22. P. Inglese, C. Saenz, C. Mondragon, A. Nefzaoui, and M. Louhaichi, *Crop Ecology, Cultivation and Uses of Cactus Pear* (FAO, 2017).

23. T. García-Cayuela, A. Gómez-Maqueo, D. Guajardo-Flores, J. Welti-Chanes, and M. Pilar Cano, "Characterization and Quantification of Individual Betalain and Phenolic Compounds in Mexican and Spanish Prickly Pear (Opuntia Ficus-Indica L. Mill) Tissues: A Comparative Study," *Journal of Food Composition and Analysis* 76 (2019): 1–13, https://doi.org/10.1016/j.jfca.2018.11.002.

24. R. Palmeri, L. Parafati, E. Arena, E. Grassenio, C. Restuccia, and B. Fallico, "Antioxidant and Antimicrobial Properties of Semi-Processed Frozen Prickly Pear Juice as Affected by Cultivar and Harvest Time," *Foods* 9, no. 2 (2020): 235, https://doi.org/10.3390/foods9020235.

25. L. Sandate-Flores, D. V. Rodríguez-Hernández, M. Rostro-Alanis, et al., "Evaluation of Three Methods for Betanin Quantification in Fruits From Cacti," *MethodsX* 9 (2022): 101746, https://doi.org/10.1016/j.mex.2022.101746.

26. K. Slinkard and V. L. Singleton, "Total Phenol Analysis: Automation and Comparison With Manual Methods," *American Journal of Enology and Viticulture* 28, no. 1 (1977): 49–55, https://doi.org/10.5344/ajev.1977.28.1.49.

27. J. Zhishen, M. Tang, and W. Jianming, "The Determination of Flavonoid Contents in Mulberry and Their Scavenging Effects on Superoxide Radicals," *Food Chemistry* 64, no. 4 (1999): 555–559, https://doi.org/10.1016/S0308-8146(98)00102-2.

28. M. W. Davey, E. Dekempeneer, and J. Keulemans, "Rocket-Powered High-Performance Liquid Chromatographic Analysis of Plant Ascorbate

and Glutathione," *Analytical Biochemistry* 316, no. 1 (2003): 74–81, [In eng], https://doi.org/10.1016/s0003-2697(03)00047-2.

29. N. Deighton, R. Brennan, C. Finn, and H. V. Davies, "Antioxidant Properties of Domesticated and Wild Rubus Species," *Journal of the Science of Food and Agriculture* 80, no. 9 (2000): 1307–1313, https://doi.org/10.1002/1097-0010(200007)80:9%3c;1307::AID-JSFA638%3e;3.0.CO;2-P.

30. D. D. Kitts, A. N. Wijewickreme, and C. Hu, "Antioxidant Properties of a North American Ginseng Extract," *Molecular and Cellular Biochemistry* 203, no. 1 (2000): 1–10, https://doi.org/10.1023/A:1007078414639.

31. R. Re, N. Pellegrini, A. Proteggente, A. Pannala, M. Yang, and C. Rice-Evans, "Antioxidant Activity Applying an Improved Abts Radical Cation Decolorization Assay," *Free Radical Biology and Medicine* 26, no. 9 (1999): 1231–1237, https://doi.org/10.1016/S0891-5849(98)00315-3.

32. A. Smeriglio, S. Bonasera, M. P. Germanò, et al., "Opuntia Ficus-Indica (L.) Mill. Fruit as Source of Betalains With Antioxidant, Cytoprotective, and Anti-Angiogenic Properties," *Phytotherapy Research* 33, no. 5 (2019): 1526–1537, [In eng], https://doi.org/10.1002/ptr.6345.

33. G. P. Studzinski, *Cell Growth and Apoptosis: A Practical Approach* (IRL Press, 1995), https://books.google.it/books?id=oFkLzgEACAAJ.

34. F. Tugba Artun, A. Karagoz, G. Ozcan, et al., "In Vitro Anticancer and Cytotoxic Activities of Some Plant Extracts on Hela and Vero Cell Lines," *Journal of Buon* 21, no. 3 (2016): 720–725, [In eng].

35. K. J. Livak and T. D. Schmittgen, "Analysis of Relative Gene Expression Data Using Real-Time Quantitative Pcr and the $2-\Delta\delta$ct Method," *Methods* 25, no. 4 (2001): 402–408, https://doi.org/10.1006/meth.2001.1262.

36. Ada, K. Milán-Noris, A. Chavez-Santoscoy Rocio, O.-N. Andrea, A. Gutiérrez-Uribe Janet, and O. Serna-Saldívar Sergio, "An Extract From Prickly Pear Peel (Opuntia Ficus-Indica) Affects Cholesterol Excretion and Hepatic Cholesterol Levels in Hamsters Fed Hyperlipidemic Diets," *Current Bioactive Compounds* 12, no. 1 (2016): 10–16, https://doi.org/10.2174/1573407212666151231183553.

37. G. Polturak and A. Aharoni, "La Vie En Rose: Biosynthesis, Sources, and Applications of Betalain Pigments," *Molecular Plant* 11, no. 1 (2018): 7–22, https://doi.org/10.1016/j.molp.2017.10.008.

38. F. Gandía-Herrero and F. García-Carmona, "Biosynthesis of Betalains: Yellow and Violet Plant Pigments," *Trends in Plant Science* 18, no. 6 (2013): 334–343, https://doi.org/10.1016/j.tplants.2013.01.003.

39. A. Smeriglio, C. De Francesco, M. Denaro, and D. Trombetta, "Prickly Pear Betalain-Rich Extracts as New Promising Strategy for Intestinal Inflammation: Plant Complex Vs. Main Isolated Bioactive Compounds," *Frontiers in Pharmacology* 12 (2021): 722398, [In eng], https://doi.org/10.3389/fphar.2021.722398.

40. S. F. H. Naqvi and M. Husnain, "Betalains: Potential Drugs with Versatile Phytochemistry," *Critical Reviews in Eukaryotic Gene Expression* 30, no. 2 (2020): 169–189, https://doi.org/10.1615/CritRevEukaryotGeneExpr.2020030231.

41. I. Gómez-López, G. Lobo-Rodrigo, M. P. Portillo, and M. P. Cano, "Ultrasound-Assisted "Green" Extraction (Uae) of Antioxidant Compounds (Betalains and Phenolics) From Opuntia stricta Var. Dilenii's Fruits: Optimization and Biological Activities," *Antioxidants* 10, no. 11 (2021): 1786, [In eng], https://doi.org/10.3390/antiox10111786.

42. V. Krajka-Kuźniak, J. Paluszczak, H. Szaefer, and W. Baer-Dubowska, "Betanin, a Beetroot Component, Induces Nuclear Factor Erythroid-2-Related Factor 2-Mediated Expression of Detoxifying/Antioxidant Enzymes in Human Liver Cell Lines," *Br J Nutr* 110, no. 12 (2013): 2138–2149, [In eng], https://doi.org/10.1017/s0007114513001645.

43. Q. Zhang, J. Pan, Y. Wang, R. Lubet, and M. You, "Beetroot Red (Betanin) Inhibits Vinyl Carbamate- and Benzo(a)Pyrene-Induced Lung Tumorigenesis Through Apoptosis," *Molecular Carcinogenesis* 52, no. 9 (2013): 686–691, [In eng], https://doi.org/10.1002/mc.21907.

44. A. Zand, S. Enkhbilguun, J. M. Macharia, et al., "Betanin Attenuates Epigenetic Mechanisms and Uv-Induced DNA Fragmentation in Hacat Cells: Implications for Skin Cancer Chemoprevention," *Nutrients* 16, no. 6 (2024): 860, https://doi.org/10.3390/nu16060860.

45. A. Saber, N. Abedimanesh, M. H. Somi, A. Y. Khosroushahi, and S. Moradi, "Anticancer Properties of Red Beetroot Hydro-Alcoholic Extract and Its Main Constituent; Betanin on Colorectal Cancer Cell Lines," *BMC Complementary Medicine and Therapies* 23, no. 1 (2023): 246, [In eng], https://doi.org/10.1186/s12906-023-04077-7.

46. A. Albergamo, A. G. Potortí, G. Di Bella, et al., "Chemical Characterization of Different Products From the Tunisian Opuntia Ficus-Indica (L.) Mill," *Foods* 11, no. 2 (2022): 155, https://doi.org/10.3390/foods11020155.

47. A. Gómez-Maqueo, T. García-Cayuela, J. Welti-Chanes, and M. Pilar Cano, "Enhancement of Anti-Inflammatory and Antioxidant Activities of Prickly Pear Fruits by High Hydrostatic Pressure: A Chemical and Microstructural Approach," *Innovative Food Science & Emerging Technologies* 54 (2019): 132–142, https://www.sciencedirect.com/science/article/pii/S1466856419300608, https://doi.org/10.1016/j.ifset.2019.04.002.

48. N. Yeddes, J. K. Chérif, S. Guyot, H. Sotin, and M. T. Ayadi, "Comparative Study of Antioxidant Power, Polyphenols, Flavonoids and Betacyanins of the Peel and Pulp of Three Tunisian Opuntia Forms," *Antioxidants* 2, no. 2 (2013): 37–51, [In eng], https://doi.org/10.3390/antiox2020037.

49. O. Hamdoun, S. Gonçalves, I. Mansinhos, et al., "Phytochemical Characterization and Bioactivity of Extracts From Different Fruit Parts of Opuntia leucotricha Dc.: A Comparison Between a Conventional Organic Solvent and Green Natural Deep Eutectic Solvents," *Horticulturae* 10, no. 8 (2024): 824, https://www.mdpi.com/2311-7524/10/8/824, https://doi.org/10.3390/horticulturae10080824.

50. L. Santos-Zea, A. M. Leal-Díaz, D. A. Jacobo-Velázquez, et al., "Characterization of Concentrated Agave Saps and Storage Effects on Browning, Antioxidant Capacity and Amino Acid Content," *Journal of Food Composition and Analysis* 45 (2016): 113–120, https://www.sciencedirect.com/science/article/pii/S0889157515002276, https://doi.org/10.1016/j.jfca.2015.10.005.

51. M. Amrane-Abider, M. Imre, V. Herman, et al., "Opuntia Ficus-Indica Peel by-Product as a Natural Antioxidant Food Additive and Natural Anticoccidial Drug," *Foods* 12, no. 24 (2023): 4403, https://doi.org/10.3390/foods12244403.

52. T. Singh, A. K. Hardeep, S. Ramniwas, et al., "Ferulic Acid: A Natural Phenol That Inhibits Neoplastic Events Through Modulation of Oncogenic Signaling," *Molecules* 27, no. 21 (2022): 7653, https://doi.org/10.3390/molecules27217653.

53. S. Quarta, N. Calabriso, M. A. Carluccio, et al., "Shielding Human Adipocytes From Inflammation: The Protective Potential of Polyphenol-Rich Opuntia Ficus-Indica Cladode Extract," *Molecular Nutrition & Food Research* 69, no. 14 (2025): e70114, https://doi.org/10.1002/mnfr.70114.

54. F. Hernández, L. Andreu-Coll, A. Bento-Silva, et al., "Phytochemical Profile of Opuntia Ficus-Indica (L.) Mill Fruits (Cv. 'Orito') Stored at Different Conditions," *Foods* 11, no. 2 (2022): 160, [In eng], https://doi.org/10.3390/foods11020160.

55. D. Daniloski, N. M. D'Cunha, H. Speer, et al., "Recent Developments on Opuntia Spp., Their Bioactive Composition, Nutritional Values, and Health Effects," *Food Bioscience* 47 (2022): 101665, https://doi.org/10.1016/j.fbio.2022.101665.

56. G. Petruk, F. Di Lorenzo, P. Imbimbo, et al., "Protective Effect of Opuntia Ficus-Indica L. Cladodes Against Uva-Induced Oxidative Stress in Normal Human Keratinocytes," *Bioorganic & Medicinal Chemistry*

Letters 27, no. 24 (2017): 5485–5489, https://doi.org/10.1016/j.bmcl.2017.10.043.

57. J. N. Rana, K. Gul, and S. Mumtaz, "Isorhamnetin: Reviewing Recent Developments in Anticancer Mechanisms and Nanoformulation-Driven Delivery," *International Journal of Molecular Sciences* 26, no. 15 (2025): 7381, https://doi.org/10.3390/ijms26157381.

58. H. S. El-Beltagi, H. I. Mohamed, A. A. Elmelegy, S. E. Eldesoky, and G. Safwat, "Phytochemical Screening, Antimicrobial, Antiaxidant, Anticancer Activities and Nutritional Values of Cactus (Opuntia Ficus Indicia) Pulp and Peel," *Fresenius Environmental Bulletin* 28, no. 2A (2019): 1545–1562, [In English].

59. S. K. Ali, S. M. Mahmoud, S. S. El-Masry, D. H. M. Alkhalifah, W. N. Hozzein, and M. A. Aboel-Ainin, "Phytochemical Screening and Characterization of the Antioxidant, Anti-Proliferative and Antibacterial Effects of Different Extracts of Opuntia Ficus-Indica Peel," *Journal of King Saud University Science* 34, no. 7 (2022): 102216, https://doi.org/10.1016/j.jksus.2022.102216.

60. E. Önem, G. Kendir, S. Akkoç, Y. Erzurumlu, M. T. Muhammed, and A. G. Özaydın, "Biochemical Contents and Antiquorum Sensing, Antiproliferative Activities of Opuntia Ficus-Indica (L.) Mill. Peel Extract," *South African Journal of Botany* 150 (2022): 296–304, https://doi.org/10.1016/j.sajb.2022.07.024.

61. A. Chimento, A. De Luca, M. D'Amico, F. De Amicis, and V. Pezzi, "The Involvement of Natural Polyphenols in Molecular Mechanisms Inducing Apoptosis in Tumor Cells: A Promising Adjuvant in Cancer Therapy," *International Journal of Molecular Sciences* 24, no. 2 (2023): [In eng], https://doi.org/10.3390/ijms24021680.

62. L. Galluzzi, I. Vitale, S. A. Aaronson, et al., "Molecular Mechanisms of Cell Death: Recommendations of the Nomenclature Committee on Cell Death 2018," *Cell Death & Differentiation* 25, no. 3 (2018): 486–541, https://doi.org/10.1038/s41418-017-0012-4.

63. A. M. Abraha and E. B. Ketema, "Apoptotic Pathways as a Therapeutic Target for Colorectal Cancer Treatment," *World Journal of Gastrointestinal Oncology* 8, no. 8 (2016): 583–591, [In eng], https://doi.org/10.4251/wjgo.v8.i8.583.

64. V. Schimek, K. Strasser, A. Beer, et al., "Tumour Cell Apoptosis Modulates the Colorectal Cancer Immune Microenvironment via Interleukin-8-Dependent Neutrophil Recruitment," *Cell Death & Disease* 13, no. 2 (2022): 113, https://doi.org/10.1038/s41419-022-04585-3.

65. S. J. Jin, Y. Yang, L. Ma, et al., "In Vivo and in Vitro Induction of the Apoptotic Effects of Oxysophoridine on Colorectal Cancer Cells via the Bcl-2/Bax/Caspase-3 Signaling Pathway," *Oncology Letters* 14, no. 6 (2017): 8000–8006, [In eng], https://doi.org/10.3892/ol.2017.7227.

66. S. Wen, X. Huang, L. Xiong, et al., "Wdr12/Rac1 Axis Promoted Proliferation and Anti-Apoptosis in Colorectal Cancer Cells," *Molecular and Cellular Biochemistry* 479, no. 12 (2024): 3341–3354, [In eng], https://doi.org/10.1007/s11010-024-04937-x.

67. D.-M. Zou, M. Brewer, F. Garcia, et al., "Cactus Pear: A Natural Product in Cancer Chemoprevention," *Nutrition Journal* 4, no. 1 (2005): 25, https://doi.org/10.1186/1475-2891-4-25.

68. F. Naselli, L. Tesoriere, F. Caradonna, et al., "Anti-Proliferative and Pro-apoptotic Activity of Whole Extract and Isolated Indicaxanthin From Opuntia Ficus-Indica Associated With Re-Activation of the Onco-Suppressor P16ink4a Gene in Human Colorectal Carcinoma (Caco-2) Cells," *Biochemical and Biophysical Research Communications* 450, no. 1 (2014): 652–658, https://doi.org/10.1016/j.bbrc.2014.06.029.

69. H. Wei, L. Qu, S. Dai, et al., "Structural Insight into the Molecular Mechanism of P53-Mediated Mitochondrial Apoptosis," *Nature Communications* 12, no. 1 (2021): 2280, https://doi.org/10.1038/s41467-021-22655-6.

70. J. M. Feugang, F. Ye, D. Y. Zhang, et al., "Cactus Pear Extracts Induce Reactive Oxygen Species Production and Apoptosis in Ovarian Cancer Cells," *Nutrition and Cancer* 62, no. 5 (2010): 692–699, [In eng], https://doi.org/10.1080/01635581003605508.

71. A. J. Levine, "P53: 800 Million Years of Evolution and 40 Years of Discovery," *Nature Reviews Cancer* 20, no. 8 (2020): 471–480, [In eng], https://doi.org/10.1038/s41568-020-0262-1.

72. D. R. Green and G. Kroemer, "Cytoplasmic Functions of the Tumour Suppressor P53," *Nature* 458, no. 7242 (2009): 1127–1130, [In eng], https://doi.org/10.1038/nature07986.

73. H. Wang, M. Guo, H. Wei, and Y. Chen, "Targeting P53 Pathways: Mechanisms, Structures and Advances in Therapy," *Signal Transduction and Targeted Therapy* 8, no. 1 (2023): 92, https://doi.org/10.1038/s41392-023-01347-1.

74. F. Abid, M. Saleem, T. Leghari, et al., "Evaluation of in Vitro Anticancer Potential of Pharmacological Ethanolic Plant Extracts Acacia Modesta and Opuntia Monocantha Against Liver Cancer Cells," *Brazilian Journal of Biology* 84 (2022): e252526, [In eng], https://doi.org/10.1590/1519-6984.252526.

75. R. Uzbekov and C. Prigent, "A Journey Through Time on the Discovery of Cell Cycle Regulation," *Cells* 11, no. 4 (2022): 704, [In eng], https://doi.org/10.3390/cells11040704.

76. G. E. Hirsch, M. M. Parisi, L. A. Martins, C. M. Andrade, F. M. Barbé-Tuana, and F. T. Guma, "Γ-Oryzanol Reduces Caveolin-1 and Pcgem1 Expression, Markers of Aggressiveness in Prostate Cancer Cell Lines," *The Prostate* 75, no. 8 (2015): 783–797, [In eng], https://doi.org/10.1002/pros.22960.

77. J. Zhu and C. B. Thompson, "Metabolic Regulation of Cell Growth and Proliferation," *Nature Reviews Molecular Cell Biology* 20, no. 7 (2019): 436–450, [In eng], https://doi.org/10.1038/s41580-019-0123-5.

78. D. Wlodkowic, J. Skommer, and Z. Darzynkiewicz, "Flow Cytometry-based Apoptosis Detection," in *Apoptosis: Methods and Protocols*, 2nd ed ed., ed. P. Erhardt and A. Toth (Totowa, NJ: Humana Press, 2009), 19–32.

79. A. T. Serra, J. Poejo, A. A. Matias, M. R. Bronze, and C. M. M. Duarte, "Evaluation of Opuntia Spp. Derived Products as Antiproliferative Agents in Human Colon Cancer Cell Line (Ht29)," *Food Research International* 54, no. 1 (2013): 892–901, https://doi.org/10.1016/j.foodres.2013.08.043.

80. N. Zaldua, F. Llavero, A. Artaso, et al., "Rac1/P21-Activated Kinase Pathway Controls Retinoblastoma Protein Phosphorylation and E2f Transcription Factor Activation in B Lymphocytes," *FEBS Journal* 283, no. 4 (2016): 647–661, https://doi.org/10.1111/febs.13617.

81. W. S. el-Deiry, J. W. Harper, P. M. O'Connor, et al., "Waf1/Cip1 Is Induced in P53-Mediated G1 Arrest and Apoptosis," *Cancer Research* 54, no. 5 (1994): 1169–1174, [In eng].

82. Y. Wang, H. Qi, Y. Liu, et al., "The Double-Edged Roles of Ros in Cancer Prevention and Therapy," *Theranostics* 11, no. 10 (2021): 4839–4857, [In eng], https://doi.org/10.7150/thno.56747.

83. H. Nakamura and K. Takada, "Reactive Oxygen Species in Cancer: Current Findings and Future Directions," *Cancer Science* 112, no. 10 (2021): 3945–3952, [In eng], https://doi.org/10.1111/cas.15068.

84. L. Gibellini, M. Pinti, M. Nasi, et al., "Interfering With Ros Metabolism in Cancer Cells: The Potential Role of Quercetin," *Cancers (Basel)* 2, no. 2 (2010): 1288–1311, [In eng], https://doi.org/10.3390/cancers2021288.

85. R. Roskoski, Jr., "The Erbb/Her Family of Protein-Tyrosine Kinases and Cancer," *Pharmacological Research* 79 (2014): 34–74, [In eng], https://doi.org/10.1016/j.phrs.2013.11.002.

86. K. P. S. Raghav and M. M. Moasser, "Molecular Pathways and Mechanisms of Her2 in Cancer Therapy," *Clinical Cancer Research* 29, no. 13 (2023): 2351–2361, [In eng], https://doi.org/10.1158/1078-0432.Ccr-22-0283.

87. Le Yu, W. Jessica, and P. Liu, "Attacking the Pi3k/Akt/Mtor Signaling Pathway for Targeted Therapeutic Treatment in Human Cancer," *Seminars in Cancer Biology* 85 (2022): 69–94, https://www.sciencedirect.com/science/article/pii/S1044579X21001887, https://doi.org/10.1016/j.semcancer.2021.06.019.

Supporting Information

Additional supporting information can be found online in the Supporting Information section. **Supporting Information.** Supporting 1. Table S1. Surrogate analytical standards and main analytical parameters for quantification of samples. Supporting 2. Figure. S1. Total ion chromatogram of purple peel extract at 16 mg/mL. Supporting 3. Table S2. Peak table related to the TIC shown in Figure S1. Supporting 4. Figure S2. Image of the original blots for p53 protein. Supporting 5. Figure S3. Image of the original blots for actin protein used as a loading control for p53 protein. Supporting 6. Figure S4. Image of the original blots for the Her2 protein. Supporting 7. Figure S5. Image of the original blots for actin protein used as loading control for Her2 protein. Supporting 8. Figure S6. Image of the original blots for the Pi3kp110 protein. Supporting 9. Figure S7. Image of the original blots for actin protein used as a loading control for Pi3kp110 protein.